Computers, Materials & Continua CMC, vol.62, no.3, pp.1303-1315, 2020

Wind-Induced Vibration Control for Substation Frame on Viscous Damper

Bingji Lan[1] and Kanghao Yan[1, *]

Abstract: In order to study the wind-induced vibration control effect of the viscous damper on the large-scale substation frame, this paper takes the large-scale 1000 kV substation frame of western Inner Mongolia as an example. The time-history sample of pulsating wind load is simulated by harmonic superposition method based on Matlab software. 6 kinds of viscous damper arrangement schemes have been designed, and SAP2000 finite element software is used for fine modeling and input wind speed time history load for nonlinear time history analysis. The displacement and acceleration of a typical node are the indicators of wind vibration control. The wind-induced vibration control effects of different schemes under different damping parameters have compared, and the damping parameters are analyzed for the optimal layout scheme. The results show that a viscous damper has installed in the lower layers of the substation; a viscous damper is placed between the ground column and the lattice beam. It is an integrated optimal solution. The wind-induced vibration control effect of the optimal scheme is sensitive to the viscous damper parameters, and the control effect does not increase linearly with the increase of the damping index and the damping coefficient. Corresponding to different damping indexes, the damping coefficient has a better range of values.

Keywords: Viscous damper, wind-induced vibration control, arrangement plan, damping coefficient, damping index.

1 Introduction

With the development of electric power industry at home and abroad, voltage levels and transmission capacity continue to increase; 1000 KV UHV substation frame is also widely used. Compared with the substation frame with relatively low voltage capacity, the 1000 KV substation frame is higher in height, which is also larger in span, more flexible and less damped. It is a typical wind-sensitive structure, and the wind load is the main control load during design. Due to the large deformation of the substation frame under wind load, large displacement and acceleration will occur along the hanging line, and a large pulling force will have generated on the wire. In order to prevent the wire breakage and ensure the safety and stability of the structure, it is necessary to control the wind of the substation frame vibration.

[1] North China University of Water Resources and Electric Power, Zhengzhou, 450045, China.

[*] Corresponding Author: Kanghao Yan. Email: xinzhongz_ncwu@163.com.

At present, the research on wind-induced vibration control of substation frames is still in the preliminary stage in the world. The research on substation frame has mainly focused on the study of wind-induced vibration coefficient, which is aiming at providing reference for design [Zhang, Zhao, Wang et al. (2017); Kalehsar and Khodaie (2018)]. However, with more and more researches on engineering numerical analysis by researchers from various countries. The accuracy of calculation results of the numerical analysis has been significantly increased, and the huge amount of calculation has been reduced [Guo, Zhuang and Rabczuk (2019); Ribeiro and Bavastri (2017)]. These approaches can be used for both forward and inverse problems and do not require a discretization.

In the wind-induced vibration control of transmission towers, passive control is widely used. This paper absorbs and dissipates vibration energy by arranging energy-consuming vibration damping devices at specific parts of the transmission tower, which helps to reduce wind-induced vibration response and improve structural reliability. Zhong et al. [Zhong, Wu and Wang (2013)] used the viscoelastic damper to displace in the upper main material of the transmission tower. The typhoon "*Qi De*" has used to dissipate the wind energy effectively, which reduced the acceleration of the top of the transmission tower by more than 60%. Zhang et al. [Zhang and Zhang (2015)] proposed to reduce the top speed and acceleration of the transmission tower by arranging the SMA damper at a specific position; however, the viscoelastic damper will add rigidity to the structure, change the natural vibration characteristics of the structure, and the viscoelastic damper is easy to age, directly increased structural maintenance costs. Although the SMA damper overcomes the characteristics of easy aging, its cost is high, and it has not been widely used in practical engineering. In this paper, different arrangement schemes of viscous dampers are selected, the optimal arrangement scheme is obtained through comparative analysis, and the combination mode of damping coefficient and damping index is further optimized in this scheme [Xu, Li and Liu (2017); Jiang, Li and Guan (2018)], so as to minimize the displacement and acceleration at the hanging point.

2 Viscous damper

As an energy dissipation and vibration-damping device, the viscous damper has a wide range of applications in the engineering field, which can protect the structure from strong wind, explosion, and ground vibration. The viscous dampers developed by Makris et al. [Makris and Constantinou (1991)] for civil engineering are speed-dependent energy consuming devices. Its mechanical behavior can have described by the following first-order Maxwell model.

$$F_d + \lambda \dot{F}_d = C_0 \dot{u} \tag{1}$$

F_d is the damping force, λ is the relaxation time coefficient, $\dot{F}_d$ is the damping force rate of change, C_0 is the zero frequency damping coefficient, and $\dot{u}$ is the relative velocity across the damping. It has been found through research that when the frequency is less than 4 Hz, the Maxwell model exhibits a frequency- independent pure viscous property, that is, $\lambda \dot{F}_d$ is negligible [Soong and Dargush (1997)]. The vibration frequency of large substation frames under wind loads is much lower than 4 Hz. Thus, Eq. (1) can have simplified to follows.

$$F_d = C_0 \dot{u} \tag{2}$$

Taylor Corporation of the United States expressed the mechanical model of a viscous damper as [Jia, Luo and Ding (2014)]:

$$F_d = C\, sgn(\dot{u})|\dot{u}|^{\alpha} \tag{3}$$

where C is the damping coefficient, sgn() is the sign function, and α is the damping index, also known as the velocity index. When $\alpha = 1$, Eq. (2) is the same as Eq. (3), which is called linear viscous damping at this time; nonlinear viscous damping at $\alpha < 1$, the damping force rises rapidly when the speed is small, and the damping growth slows as the speed increases. When $\alpha > 1$ is the lock damping, its damping effect is opposite to the nonlinear viscous damping, and the damping force grows faster at higher speeds.

The substation frame is a long-span and high-flexibility structure. When it has exposed to wind loads for a long time, the deformation rate of the member is relatively small, considering that the energy dissipation performance of the viscous damper should have fully exerted. Therefore, it is reasonable to take $\alpha < 1$ to obtain nonlinear viscous damping. The viscous damper only provides additional damping for the structure without increasing the structural stiffness, so the frequency characteristics of the structure have not changed by the addition of the viscous damper, the economy is good, and the purchase and maintenance costs are relatively low.

3 Project overview and finite element model

3.1 Project overview

The 1000 kV high-voltage substation is located in the western part of Inner Mongolia and belongs to a three-span large-scale substation. This substation structure consists of four lattice towers: Z1, Z2, Z3, Z4. And it consists of three lattice beams：L1, L2, L3. The height of the lattice column is 56 m, the height of the ground column is 11.5 m, the span of the lattice beam is 53 m, the beam height is 3 m, and the elevation of the beam bottom is 41.5 m. All components of the substation frame are made of thin-walled round steel tubes of Q345. The two-dimensional view of the structure is shown in Fig. 1.

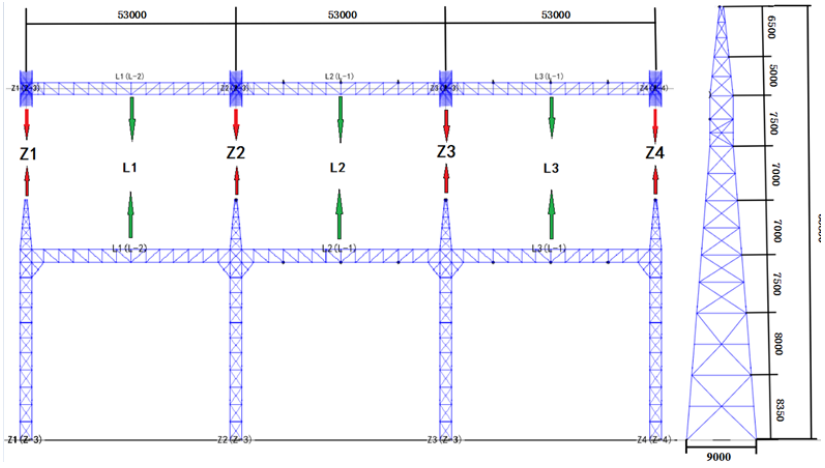

Figure 1: Structure of substation tower

The coordinate axes have defined as follows, the X direction is the direction of the beam, the Y direction is the vertical beam direction, and the Z direction is the vertical direction; the wind direction angle is defined as follows, the vertical beam direction is 0° wind direction angle, and the straight beam direction is 90° wind direction angle.

3.2 Architecture finite element model

The finite element modeling of the structure has carried out using SAP2000 finite element software. The framework has modeled using framework elements, which have modeled by 584 nodes and 1644 units. The overall model and the foundation are considered to consolidate. The finite element model is shown in Fig. 2.

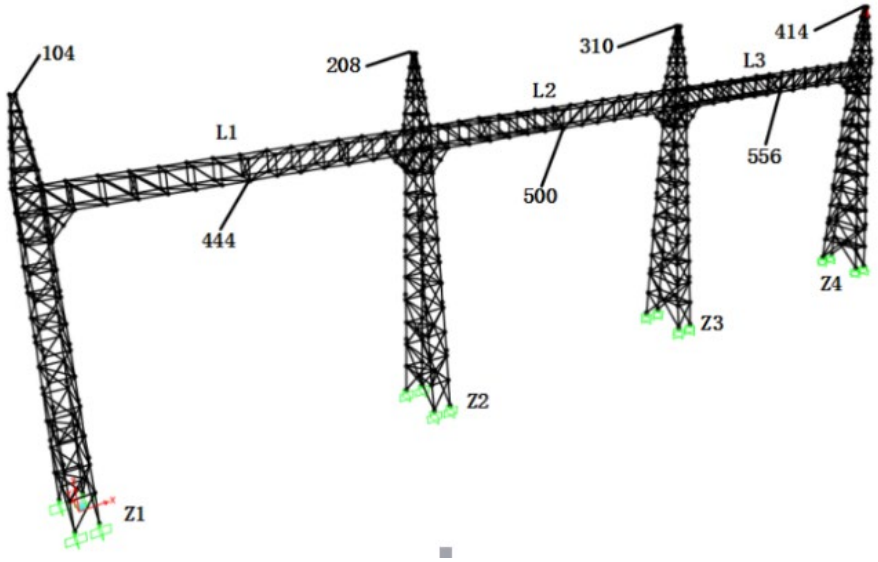

Figure 2: Finite element model of transformer tower

4 Wind load numerical simulation

In this paper, the harmonic superposition method is used to simulate the wind load. The pulsating wind has simulated by Kaimal spectrum. The maximum wind speed at 10 m height is 31.12 m/s, the Kaman length is 0.4, the spatial correlation function coefficient is 10, and the wind speed duration of each group is 150 s, the time interval is 0.15 s, and the air density is 1.293 kg/m^3. In this paper, the simulated wind speed of each lattice tower 6-elevation point has simulated by Matlab, each lattice beam has divided into four sections according to the span, and the wind speed time history of three junction points is simulated and 33 wind speed time-course samples are obtained. It has converted into wind pressure applied to the corresponding position of the frame [Xu (2010)].

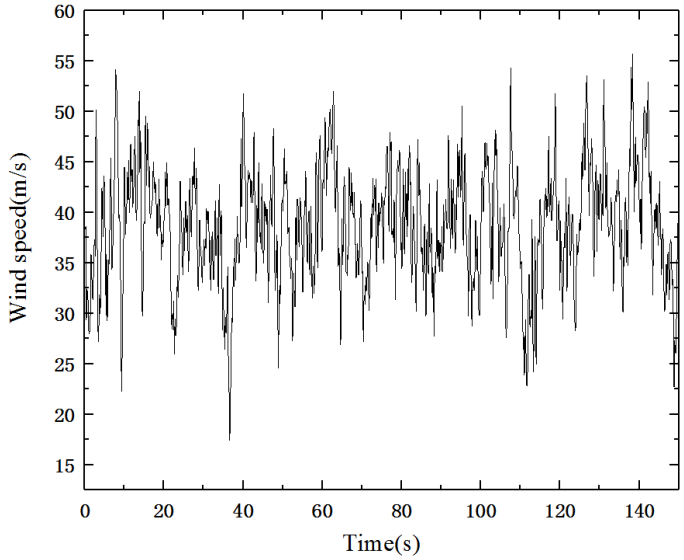

Figure 3: Simulated wind speed time history at Z4 lattice tower height of 49.5 m

5 Damper layout scheme comparison

In the research of wind-induced vibration of the substation frame, the response of the frame under wind load is studied under the condition of 0° wind direction angle (Y direction), 90° wind direction angle (X direction) and 45° wind direction angle between them. Among the three wind direction angles, the X and Y displacements of the structure are in the same order of magnitude at the 45° wind direction angle [Chen, Chen and Zheng (2011); Pan, Tong and Sheng (2009); Yang, Wang and Wang (2010)], and the damping control effect of the control scheme in the X and Y directions can be observed simultaneously. Therefore, the 45° wind direction angle has taken in this paper, and the control effect of the viscous damper on the wind-induced vibration of the substation frame is studied. The X and Y direction deformation and acceleration of the frame will generate additional tension on the wire. When the wire is broken during the operation of the substation structure, the displacement and acceleration of the control line are the main targets of wind vibration control. The damping index is as follows:

$$\eta_n = \frac{\rho_{u,max} - \rho_{r,max}}{\rho_{u,max}} \tag{6}$$

$$\eta_\alpha = \frac{\beta_{u,max} - \beta_{r,\max}}{\beta_{u,max}} \tag{7}$$

η_n and η_α are the displacement damping rate and the acceleration damping rate respectively. $\rho_{u,max}$ and $\beta_{u,max}$ are the absolute values of the peak displacement and the peak acceleration of the uncontrolled structural node, respectively. $\rho_{r,max}$ and $\beta_{r,max}$ are the absolute values of the peak displacement and the peak acceleration of the device after the viscous damper.

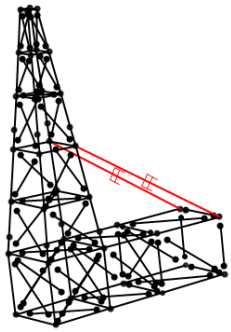

(a) One-way tower beam arrangement

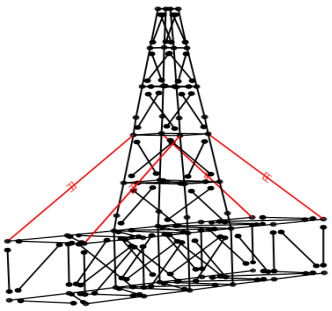

(b) Two-way tower beam arrangement

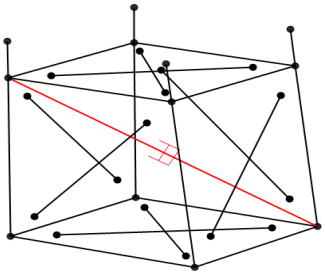

(b) Single layer arrangement

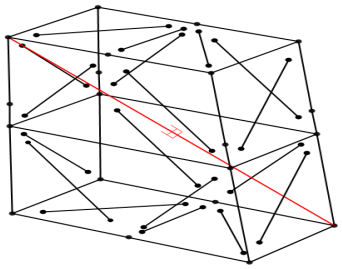

(d) Double layer arrangement

Figure 4: Schematic diagram of damper arrangement

The setting position of the viscous damper and the damper parameters has obvious influence on the structure damping effect. Therefore, 6 damper arrangement position schemes are selected in this paper, and the damping coefficient and damping index are optimized for each scheme. The scheme of damper arrangement is shown in Fig. 6. and Tab. 1. Since the Z1 and Z4 towers have symmetrically arranged, the Z2 and Z3 towers have symmetrically arranged. Therefore, only the Z1 and Z2 tower layout methods are shown in the figure, and the main frame and the lateral bracing are hidden. For easy identification. Fig. 5(a) is the full method. As the control group, 60 viscous damping units with the same parameters have set in the frame. Figs. 5(b)-5(f) all use 32 damping units with the same parameters, that is, each tower has 8 grids. Tab. 1 details the layout of each damper arrangement position scheme. For each scheme, the damping coefficients are 50,000, 100,000, 200,000, 300,000, 400,000, 500,000, 600,000, 700,000, and 800,000$N \cdot (m/s)^{-1}$ respectively, and the damping indices have taken as 0.15, 0.3, 0.45, 0.6, 0.75, and 1. In addition, the displacement-damping rates and acceleration-damping rates of node 310 and node 556 are selected as vibration reduction index to research the relationship between damper arrangement position schemes and the effect of vibration control.

(a) Overlay method

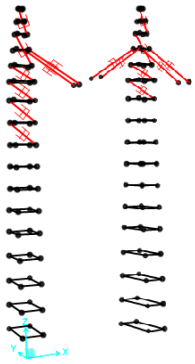

(b) Upper layout method 1

(c) Upper layout method 2

(d) Lower layer layout method

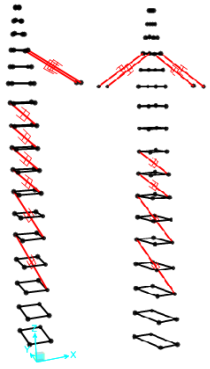

(e) Middle layout method

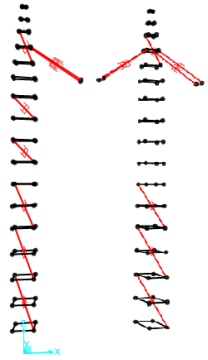

(f) Interlayer layout method

Figure 5: 6 kinds of damping arrangement

Table 1: position of dampers

Program	Arrangement position
Full cloth	All lattice towers have a single layer arrangement if there is a web among the layers, and if there is no web, there is a double layer arrangement. A tower beam arrangement is used among all ground posts and beams.
Upper layout method 1	The Z1 and Z4 lattice towers have arranged in a single layer from the 10th floor with the webs, and the double layer is arranged if there is no web. The Z2 and Z3 lattice towers have arranged in a single layer from the 12th floor with the webs, and the double layer is arranged if there are no webs. A tower beam arrangement is used among all ground posts and beams.
Upper layout method 2	All lattice towers have arranged in a single layer from the 8th floor if there is a web among the layers, and if there is no web, there is a double layer arrangement.
Lower arrangement	The 1st and 9th floors of the Z1 and Z4 lattice towers have arranged in a single layer with the webs, and the double layer is arranged if there are no webs. The Z2 and Z3 lattice towers have arranged in a single layer from the 1st to 7th floors with the webs, and the double layer is arranged if there is no web. A tower beam arrangement is used among all ground posts and beams.
Central arrangement	The 4th floors of the Z1 and Z4 lattice towers have arranged in a single layer with the webs, and the double layer is arranged if there are no webs. The Z2 and Z3 lattice towers have arranged in a single layer from the 4-9 floors with the webs, and the double layer is arranged if there are no webs. A tower beam arrangement is used among all ground posts and beams.
Interval layout	Z1, Z4 lattice towers 2-7, 14-15 layers have arranged in two layers, and 9 and 11 layers have arranged in a single layer. The Z2 and Z3 lattice towers have arranged in two layers from 2-7 and 14-15 floors. A tower beam arrangement is used among all ground posts and beams.

Tab. 2 shows the comparison of typical node damping effects and the typical node motion when the control schemes have optimal damping parameters. In this paper, by comparing the results of the above different layout schemes, the upper layout method 1 has a displacement damping ratio greater than 14%, and an acceleration damping ratio is greater than 15% in the X direction of the selected node. Compared to the upper arrangement method 2 apparently in X. There is better damping effect in the direction, but the displacement of the two upper arrangements in the Y direction and the acceleration control effect are not obvious. This paper describes a viscous damper placed between the grounding column and the lattice beam, which can significantly control the

displacement and acceleration peak of the frame in the X direction. At the same time, it can be shown that the provision of a viscous damper on the upper part of the lattice tower is of little significance for wind-induced vibration control in the Y direction. Compared with the full-distribution method, the lower-layer arrangement method has little difference in displacement damping rate and acceleration damping rate, but it has a slight advantage in damping ratio compared with the interlayer arrangement method and the central arrangement method, and is also arranged with two kinds of upper parts. The method has obvious advantages. This is because the structural deformation is mainly concentrated in the lower part, and the damper has arranged in the middle and the upper part because the structural deformation is small, and the relative displacement at both ends of the damper is small, which affects the energy consumption effect. The lower layer arrangement method is more prominent in the vibration damping effect, and is relatively economical because it uses fewer damping elements than the full cloth method. At the same time, since the damper is mainly concentrated in the lower part of the structure for easy replacement and maintenance, the upper and lower layer layout method should be the optimal layout scheme.

Table 2: Optimal damping parameters and damping effects of each scheme

Vibration reduction scheme	Node NO.	Damping coefficient $/N \cdot (m/s)^{-1}$	Damping index α	X-direction displacement damping rate $\eta_u/\%$	Y-direction displacement damping rate $\eta_u/\%$	X-direction acceleration damping rate $\eta_\alpha/\%$	Y-direction acceleration damping rate $\eta_\alpha/\%$
Full cloth	310	700000	0.45	22.3	9.5	43.9	13.7
	556			13.7	6.6	41.8	25.8
Upper layout method 1	310	700000	0.15	22.0	0	15.7	4.4
	556			14.2	2.8	23.4	3.5
Upper layout method 2	310	50000	0.15	1.5	5.4	7.5	4.7
	556			3.7	1.7	9.6	10.8
Central arrangement	310	500000	0.3	21.7	6.9	32.2	4.1
	556			18.4	1.1	35.2	14.5
Lower arrangement	310	300000	0.3	21.1	9.9	36.1	12.7
	556			18.2	6.6	40.5	22.9
Interval layout	310	800000	0.3	22.8	6.0	31.3	2.9
	556			18.4	0	31.6	13.2

6 Influence of 5 parameters on wind turbine vibration control of optimal scheme

From the above analysis, the optimal scheme of wind-induced vibration control is the lower layout method, and the damping effect varies with the damping coefficient and the damping index, as shown in Fig. 6-Fig. 13.

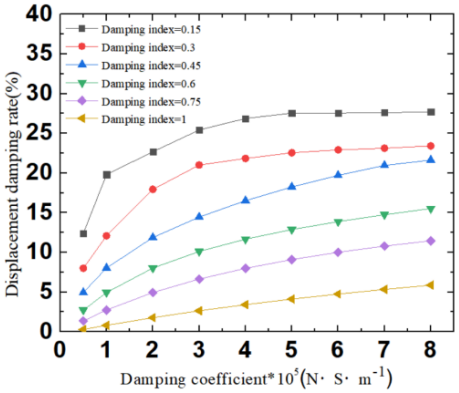

Figure 6: Structure 310 node X-direction displacement damping rate

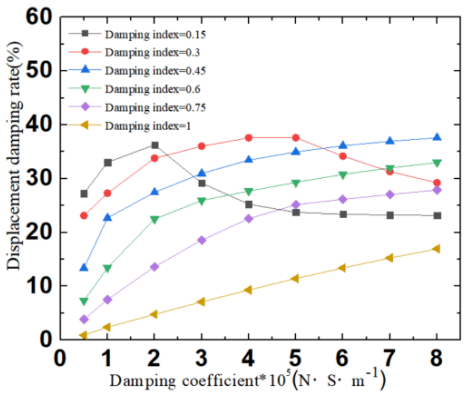

Figure 7: Structure 310 node X-direction acceleration damping rate

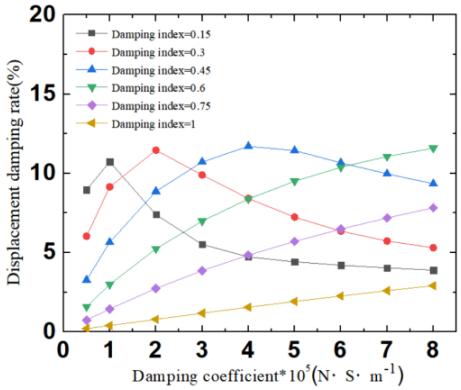

Figure 8: Structure 310 node Y-direction displacement damping rate

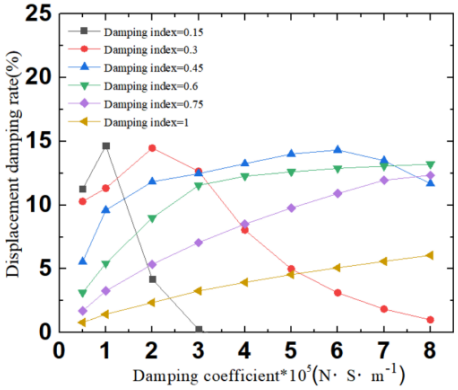

Figure 9: Structure 310 node Y-direction acceleration damping rate

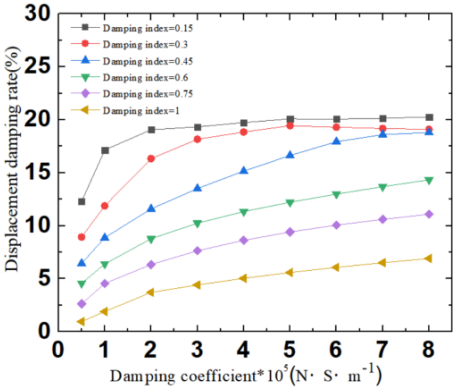

Figure 10: Structure 556 node X-direction displacement damping rate

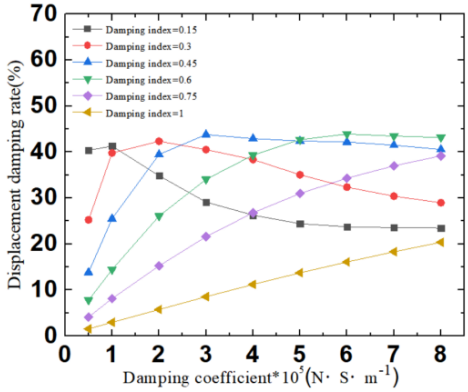

Figure 11: Structure 556 node X-direction acceleration damping rate

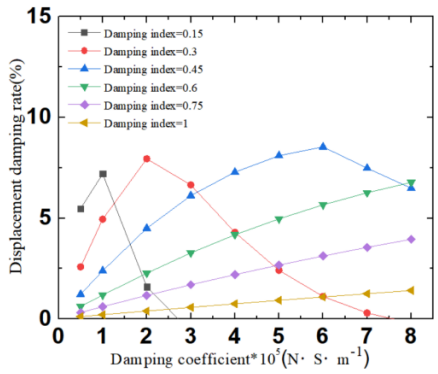

Figure 12: Structure 556 node Y-direction displacement damping rate

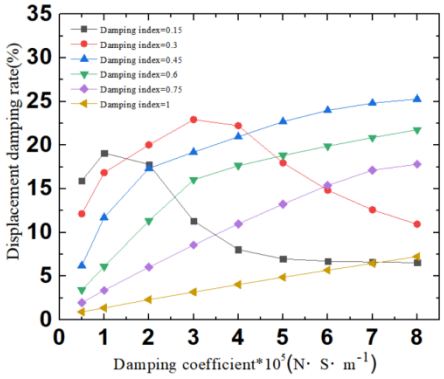

Figure 13: Structure 556 node Y-direction acceleration damping rate

It can be seen from the damping effects of the 310 and 556 nodes in the above figure that when the damping index of the viscous damper is small, for example, 0.15 and 0.3 are selected, both damping rates reach the maximum value of 100,000~400,000 $N \cdot (m/s)^{-1}$, and the maximum value is ideal. With the increase of the damping coefficient, the displacement damping rate and the acceleration-damping rate will gradually decrease. When the damping coefficient is large, the displacement damping rate and the acceleration-damping rate will even be lower than the damping coefficient at 50,000 $N \cdot (m/s)^{-1}$. Therefore, the damping coefficient has selected, which is not too big. When the damping index selects intermediate values such as 0.45 and 0.6, the displacement and acceleration-damping rate will gradually increase with the increase of damping coefficient. In general, the damping effect tends to be stable after 600,000 $N \cdot (m/s)^{-1}$ and the damping effect is ideal. It is almost the same as the optimum value of the damping rate when the damping index is small. When the damping index is large, for example, when 0.75 and 1 are selected, the damping effect tends to increase with the damping coefficient, but the overall effect is not good, because the damping index is larger, the deformation of the limit damper has displaced, resulting in no damping effect well.

7 Conclusion

The wind-induced vibration response of the frame has studied by placing a viscous damper at different positions of the substation frame and adjusting the damper parameters. The results are as follows:

(1) Viscous damper has obvious effect on wind-induced vibration control of large-scale substation frame, especially for X-direction displacement and acceleration control. The maximum damping rate of X-direction displacement and acceleration at the top node of grounding column can reach 22.3% and 43.9%. The maximum damping rate of the displacement and acceleration of the X-direction displacement of the lattice beam is 19.6% and 41.8%, and the control effect is quite different when using different layout schemes.

(2) Among the six methods of viscous dampers, the lower layout method and the full cloth method have the best control effect, and the two layout methods have similar

control effects, but because the lower arrangement method is convenient to install and economical and feasible, For the best layout.

(3) The parameter analysis results based on the bottom arrangement method show that the damping index not used for the viscous damper has different damping coefficient better value range. When the damping coefficient is smaller, the damping coefficient should not have chosen to be large. Moreover, when the damping index is close to 1, close to linear damping, the structural damping effect is not obvious.

(4) There is a big difference between the two upper layout methods in the X-direction wind vibration control effect, mainly because the viscous damper disposed between the ground column and the lattice beam has a significant energy consumption effect, and the viscous damper is arranged. It is a good choice between the grounding column and the lattice beam.

Conflicts of Interest: The authors declare that they have no conflicts of interest to report regarding the present study.

References

Chen, W.; Chen, C. X.; Zheng, W. (2011): Calculation of wind vibration coefficient of 1000kV substation frame. *Electric Power Construction*, vol. 32, no. 9, pp. 30-32.

Guo, H. W.; Zhuang, X. Y.; Rabczuk, T. (2019): A deep collocation method for the bending analysis of Kirchhoff plate. *Computers, Materials & Continua*, vol. 59, no. 2, pp. 433-456.

Jia, B.; Luo, X. Q; Ding, J. (2014): Study on damping effect of viscous damper on space truss structure. *Journal of Vibration and Shock*, vol. 33, no. 6, pp. 124-130.

Jiang, Y.; Li, J.; Guan, Z. (2018): Shake table studies on viscous dampers in seismic control of a single-tower cable-stayed bridge model under near-field ground motions. *Journal of Earthquake and Tsunami*, vol. 12, no. 5, pp. 11-22

Kalehsar, H. E.; Khodaie, N. (2018): Wind-induced vibration control of super-tall buildings using a new combined structural system. *Journal of Wind Engineering & Industrial Aerodynamics*, vol. 172, no. 1, pp. 256-266.

Makris, N.; Constantinou, M. C. (1991): Fractional-derivative Maxwell model for viscous dampers. *Journal of Structural Engineering*, vol. 117, no. 9, pp. 2708-2724.

Pan, F.; Tong, J. G.; Sheng, X. H. (2009): Study on wind-induced vibration response of 1000kV large-scale thin-walled steel tube substation frame. *Engineering Mechanics*, vol. 26, no. 10, pp. 203-210.

Ribeiro, E. A.; Bavastri, C. A. (2017): A numerical and experimental study on optimal design of multi-DOF viscoelastic supports for passive vibration control in rotating machinery. *Journal of Sound Vibration,* vol. 411, no. 1, pp. 346-361.

Soong, T. T; Dargush, G. F. (1997): Passive energy dissipation systems in structural engineering. *Structural Safety,* vol. 20, no. 2, pp. 197-198.

Xu, Z. D. (2010): *Analysis and Application of Common Software for Civil Engineering.* China Building Industry Press.

Xu, X.; Li, Z.; Liu, W. (2017): Investigation of the wind-resistant performance of seismic viscous dampers on a cable-stayed bridge. *Engineering Structures*, vol. 145, no. 1, pp. 283-292.

Yang, M.; Wang, W.; Wang, L. (2010): Study on wind load effect of 1000kV fully integrated substation frame. *Journal of Wuhan University (Engineering Science)*, vol. 1, no. 1, pp. 100-104.

Zhang, C. R.; Zhang, F. (2015): Wind-induced vibration control of transmission tower based on SMA damper. *Science & Technology Review*, vol. 33, no. 7, pp. 74-78.

Zhong, W. L.; Wu, L. L.; Wang, W. (2013): Wind-induced vibration suppression method for high-voltage transmission tower based on damping energy dissipation principle. *Journal of Central South University (Natural Science)*, vol. 44, no. 1, pp. 397- 402.

Zhang, M.; Zhao, G. F.; Wang, L. L.; Li, J. (2017): Wind-induced coupling vibration effects of high-voltage transmission tower-line systems. *Shock and Vibration*, vol. 2017, no. 4, pp. 1-34.